Chemical composition of chromite and intergrown chlorite in metamorphosed ultramafic rocks (serpentine and talc schsit) of the Egbe–Isanlu schist belt, southwest Nigeria: genetic i...

Article *in* Journal of Mining and Geology · January 2011

CITATIONS
0

READS
51

1 author:

Samuel Bamidele Olobaniyi
University of Lagos
40 PUBLICATIONS **366** CITATIONS

SEE PROFILE

Journal of Mining and Geology Vol. 47(2) 2011, pp. 115-134 1116-2775

Chemical composition of chromite and intergrown chlorite in metamorphosed ultramafic rocks (serpentinite and talc schist) of the Egbe-Isanlu schist belt, southwest Nigeria: genetic implications

Samuel B. Olobaniyi[*] and Arno Mücke[**]

[*] Department of Geology, Delta State University, Abraka, Delta State, Nigeria

e-mail: sbolobaniyi@yahoo.com

[**]Abteilung Mineralogie, Geowissenschaftliches Zentrum, Georg-August-Universitat

37077 Göttingen, Goldschmidtstrasse 1, Germany

e-mail: arhemucke@gmx.de

Abstract

In the Egbe-Isanlu schist belt serpentinite of dark and light greenish colours and whitish-grey talc schist occur. In these rocks black spots consisting of chromite are disseminated. Chromite is always intimately intergrown with chlorite . In serpentinite, chromite occurs first as compact and irregular crystals (up to 200 ìm) that may be associated with magnetite, ilmenite and sulphides or secondly as tiny crystals (5 ìm or smaller) which are concentrated within rectangular to rounded shaped outlines that represent the original shape of chromite grains. The latter type is predominantly developed in talc schist where tiny chromite crystals arranged in the herringbone structure are of subordinate abundance. The main end-members of the chromite solid solutions in serpentinite and talc schist are $FeCr_2O_4$ *(= **chromite)** and* $Fe^{2+}Fe^{3+}{}_2O_4$ *(= magnetite) with the chromite-magnetite **mole** ratios generally higher in talc schist than serpentinite. Chlorite has the composition of clinochlore and shows low level of chemical variability. However,* Cr_2O_3 *and NiO occur in anomalously enhanced concentrations. Thermometric calculations suggest that chlorite was formed or re-equilibrated within the greenschist metamorphic spectrum. This investigation revealed that, chromite originally contained in ultramafic rocks (= peridotite), inferred to be similar in composition to chromite of stratiform deposits, suffered chemical alterations during metamorphism. The original peridotite was transformed into serpentinite and talc schist while the altered chromite suffered a near complete loss of Al and Mg and the enrichment of Cr, Ti, Zn and Fe-concentrations.*

Introduction

Generally, chromite occurs in ultramafic and mafic plutonic igneous (dunite, peridotite, harzburgite, pyroxenite, norite and gabbro) as well as in extrusive rocks (e.g. basalts and komatiite). Chromite may also occur in altered and metamorphosed rocks (e.g. serpentinite and talc schist), the protoliths of which are the above mentioned igneous and extrusive rocks. In economic concentrations, however, chromite is either related to intrusive systems in cratonic settings (1) or to orogenic zones (2), often located along oceanic spreading centres associated with ophiolite. Chromite enrichments of type (1) are known as stratiform deposits, whereas those of type (2) occur in podiform deposits. The latter type is also known as the ophiolite-Alpine peridotite type (Guilbert and Park, 1985).

Chromite belonging to the spinel group has the formula $Fe^{2+}Cr_2O_4$ and can show a considerable variation in composition with magnesium substituting for ferrous iron and aluminium and/or ferric iron substituting for the chromium. Due to this compositional variation, chromites in different geological settings have distinct compositions and thus can be differentiated from one another. Chromite from stratiform deposits, has high Cr and low Al concentrations (Cr-number 60 to 80), whereas those of Mg and Fe^{2+} vary over a wide range (Mg-number 20 to 80). Chromite from podiform deposits may have distinctly lower Cr-numbers and thus higher Al and Mg concentrations (Cr-number: 15-85; Mg-number 40-80)(Steele *et al.,* 1977). Chromite apart from its economic significance is widely recognized as potentially important petrogenetic indicators (Barnes and Hills, 1995; Arif and Jan, 2006). However, this attribute is often limited by compositional alterations arising from post-crystallization re-equilibrum and metamorphic alterations (Roeder and Campbell, 1985; Burkhard, 1993). Therefore studying the mechanism of metamorphic alteration and chemical patterns is critical to assessing the applicability of

*Corresponding author: sbolobaniyi@yahoo.com

chromites to petrogenetic reconstructions in metaultramafic rock (Abzalov, 1998).

The occurrence of chromite in ultramafic rocks within the Nigerian Basement Complex has been reported (Wright and Ogezi, 1977; Onyeagocha, 1979; Muecke and Woakes, 1986; Baer and Glaeser, 1988) but apart from Muecke and Woakes (1986), no detailed account of the chemical characteristics of chromite is available. This paper presents the petrology and chemical composition of chromite and associated chlorite in serpentinized and talcitized ultramafic rocks of the Egbe-Isanlu schist belt and discusses the modification to chromite chemistry. This contribution is specifically significant to the mechanism of secondary chromite formation.

Geological setting

The Nigerian Basement Complex consists of Precambrian gneiss and migmatitic rocks. Into these are infolded about 14 low to medium grade supracrustal dominated schist belts (Ajibade *et al.* 1987) of probable Archean to Proterozoic age (Olobaniyi and Annor, 2003; Muecke, 2005). The belts are North-Southerly trending and are dominantly restricted to the western half of Nigeria in a zone of about 1000 km in length and 600 km width (Fig. 1). The supracrustals consist of pelitic to semipelitic and quartzitic schists, interlayered with relatively minor horizons of carbonate, banded iron-formation as well as mafic to ultramafic rocks including their altered equivalents serpentinite and talc schist (Olobaniyi and Annor, 2003). Both, basement and supracrustal cover sequences have suffered polyphase deformation and metamorphism and are intruded in places by Pan-African granitoids.

Although meta-mafites and meta-ultramafites are relatively minor components of the Nigerian basement complex, they have been identified and studied in some schist belts of Nigeria. Examples of these include the Ilesha (Elueze, 1981 and 1982; Kayode, 1981; Klemm *et al.,* 1984; and Ige and Asubiojo, 1991), Kusheriki (Truswell and Cope, 1963), Egbe-Isanlu (Olobaniyi and Annor, 2003; Olobaniyi, 2006 and 2008), Maru (Elueze 1982), Wonaka and Anka (Ogezi, 1977:Wright and Ogezi, 1977; Muecke and Woakes, 1986; Muecke, 2003) and Malumfashi (Baer and Glaeser 1988; Ogezi, 1988) schist belts . Conclusions from some of these studies have suggested that the pre-metamorphic parentage of these rocks are magmatic (Ige and Asubiojo, 1991) and identical to peridotite (Elueze, 1982) or to Mg-rich komatiite (Olobaniyi and Annor, 2003).

The Egbe-Isanlu schist belt is one of the N-S trending Proterozoic basins. It lies in the southwest of Nigeria and about 100 km east of Ilorin (Fig. 1). The belt is dominated by semi-pelitic schists that are interbanded with other lithologies including quartzite, banded iron-formation, serpentinite, talc schist and amphibolite (Annor et al., 1997, Olobaniyi, 1997; Fig. 2). These rock units bear similar structural imprints and show mineral assemblages that imply metamorphism within the greenschist to mid-amphibolite facies conditions (Olobaniyi, 1997). The metamorphic sequence is intruded in places by the Pan-African Older Granites (Fig. 2). Talc schists and serpentinite within the Egbe-Isanlu schist belt occur as low-lying sheets and lenses within the meta-sediments of the area, concentrated in the upper part of the map area. The schists are more than 3 km in width and located around the villages of Odogbe and Ilafin, and define a band that passes through Okolom to the north. The original ultramafic rock is not preserved, but has been transformed into serpentinite and talc schist (Fig. 2). Therefore, the mineral assemblages are either dominated by serpentine (antigorite) that may be associated with chlorite, tremolite, talc and calcite or talc, antophyllite, chlorite, phlogopite, magnesite and subordinate antigorite. Both assemblages also contain chromite that constitute about 1 2 % of the rock volume (Olobaniyi and Annor, 2003).

Methods

Electron-microprobe analyses

For this study, about 30 samples were available. However, only some of them contain chromite grains, in sizes that are big enough for electron-microprobe analysis. Four rock samples that represent the range of rocks studied and contain chromite of suitable grain sizes were selected for analysis. The chromite crystals occasionally contain narrow higher reflecting rims, which are usually too small to analyze. Therefore, electron-microprobe analyses were carried out mainly in the centre of the grains. In all, 46 chromite and 22 other mineral analyses (chlorite, magnetite and ilmenite) were carried out. Many of them are chemically nearly identical or similar. Therefore, 20 chromite (2 from the rim), three magnetite, and 10 chlorite analyses were selected for publication which all represents the whole chemical span of each mineral.

Electron-microprobe analyses were carried out at the Abteilung Geochemie of the Göttinger Zentrum

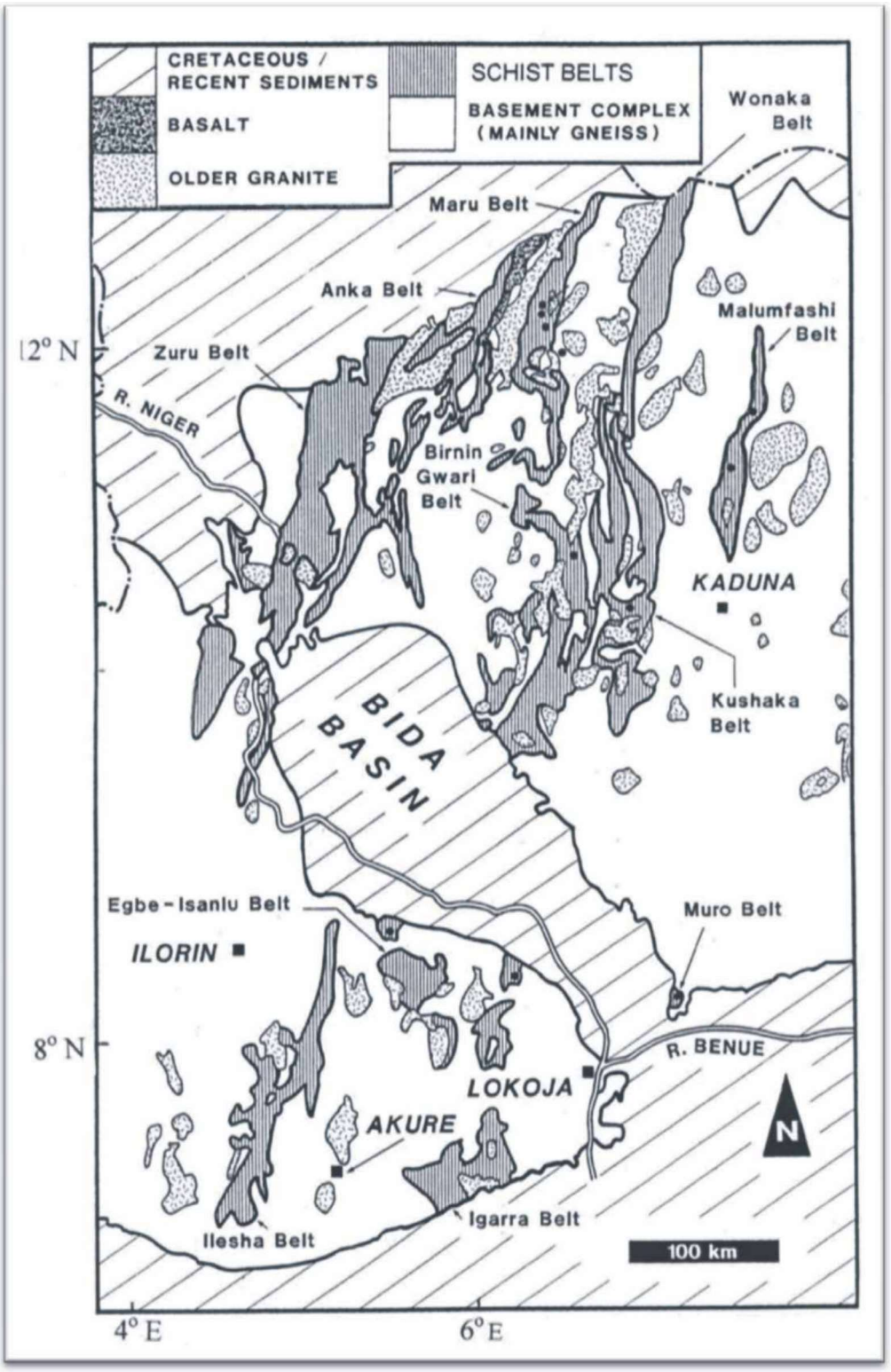

Fig. 1: Geological map of the western sector of Nigeria showing the distribution of metavolcano-metasedimentary schist belts including the Egbe-Isanlu belt and the Older Granites (from Mücke, 2005).

für Geowissenschaften, Germany. Wavelenght-dispersive microprobe analyses were performed using JEOL instrument equipped with five WDS detectors. For quantitative measurement, 15 kV acceleration voltage, 20 nA current on the Faraday cup and 5 ìm defocused beam were chosen. Counting times ranged between 12 and 22 s on the peak. The following standards were used for the analyses: wollastonite, MgO, TiO_2, Cr_2O_3, rhodonite, hematite, NiO, V, Al_2O_3 and gahnite.

Calculation of mineral-formulae

The analytical data of **chromite/magnetite** (Tables 1 and 2, part A; in wt. %) were transformed into at. % on the basis of three cations (Tables 1 and 2, part B). From the latter data, the corresponding end-member concentrations were deduced (Tables 1 and 2, part C; in mol. %). The proportions of Fe^{2+} and Fe^{3+} were determined on the basis of electroneutrality for the formula, considered under part B (Table 1 and 2) and finally transformed into wt. % expressed as FeO_{calc} and Fe_2O_{3calc}. These were added to the analytical sum instead of FeO_{anal} (Tables 1 and 2, part A).

Chlorite analyses (Table 3, part A; in wt. %) were calculated on the basis of 10 cations including minor CaO, Na_2O and K_2O. Two assumptions were made in the electroneutrality calculation of chlorite formula $(Fe^{2+},Mg,Fe^{3+},Al)_6[OH)_8/(Si,Al)_4O_{10}]$:

1. The sum of the valances of the anions (= 28) is higher than the sum of the valences of the cations (with the assumption that iron is exclusively Fe^{2+}). The excess of negative charge is compensated by the introduction of a certain amount of Fe^{3+} (Table 3, part B, analyses I, IV, V and VII-IX; in apfu).
2. The sum of the valances of the anions (= 28) is lower than the total of the valences of the cations (with the assumption that iron is exclusively Fe^{2+}). The deficiency of negative charges is compensated by the introduction of O^{2-} instead of OH^-. (Table 3, part B, analyses II, III, VI and X; in apfu).

The amount of water (in the form of OH^-) was deduced from the formulae (containing 8 OH^-,

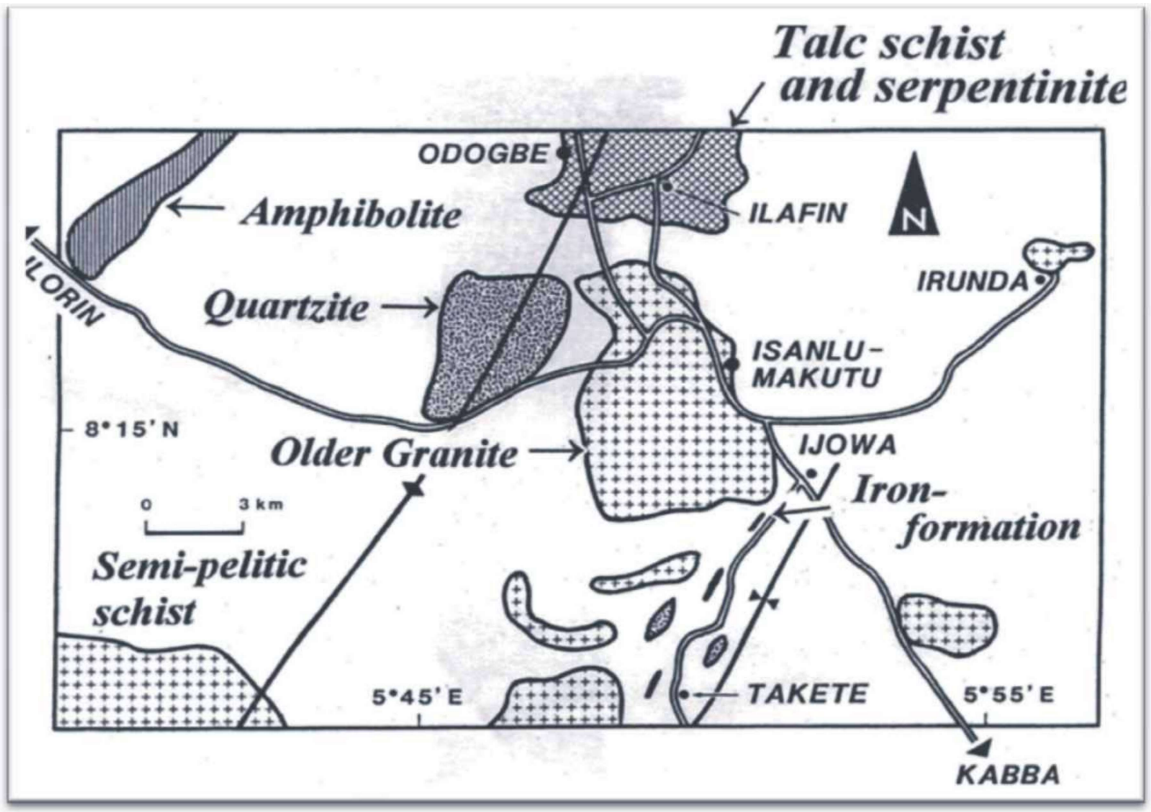

Fig. 2: Geological map of the Isanlu area showing the dominating semi-pelitic schist in which other rocks are enclosed [(talc schist and serpentinite), amphibolite, quartzite, iron-formation and Older Granite) (from Annor et al., 1997)].

Table 1: Chemical composition of chromite and magnetite in serpentinite

	Serpentinite-sample SB 9					Serpentinite-sample NT 76					
	Chromite								Magnetite		
	I	II	III	IV	V	VI	VII	VIII	IX	X	XI
A: Weight-percent (wt. %)											
SiO_2	n.d.	n.d.	n.d.	0.08	0.06	n.d.	n.d.	n.d.	n.d.	n.d.	N.d.
TiO_2	1.78	2.13	2.33	3.29	4.03	3.28	2.54	2.89	2.35	0.13	0.09
Al_2O_3	0.59	0.54	0.51	0.37	0.30	0.36	0.32	0.35	0.26	n.d.	-
Cr_2O_3	43.47	41.74	40.03	37.60	33.29	38.57	36.88	35.46	29.73	1.07	0.38
V_2O_3	0.25	0.26	0.28	0.32	0.36	0.22	0.21	0.22	0.20	n.d.	-
FeO_{anal}	49.88	50.76	52.06	53.89	56.63	52.58	53.91	55.78	62.68	90.62	92.68
MnO	1.29	1.32	1.19	0.90	1.14	0.69	0.60	0.60	0.47	n.d.	N.d.
NiO	0.05	0.07	0.06	0.09	0.10	0.14	0.16	0.17	0.17	0.17	0.20
ZnO	0.89	0.83	0.80	0.64	0.62	1.07	1.13	0.95	0.77	n.d.	N.d.
MgO	0.35	0.32	0.30	0.19	0.23	0.37	0.32	0.33	0.27	0.30	0.07
FeO_{calc}	30.98	31.17	31.43	32.75	32.99	32.24	31.31	31.98	32.10	30.26	31.63
Fe_2O_{3calc}	21.00	21.78	22.93	23.49	26.28	22.61	25.12	26.45	33.98	67.09	66.74
Σ	***100.65***	***100.19***	***99.86***	***99.64***	***99.34***	***99.55***	***98.59***	***99.40***	***100.30***	***99.02***	***99.22***
B: Atoms per formula unit (apfu)											
Ti	0.050	0.060	0.066	0.093	0.115	0.093	0.073	0.082	0.067	0.004	0.003
Al	0.026	0.024	0.023	0.017	0.013	0.016	0.014	0.016	0.012	-	-
Cr	1.279	1.235	1.189	1.121	0.997	1.150	1.112	1.060	0.885	0.033	0.012
V	0.007	0.008	0.008	0.010	0.011	0.007	0.007	0.007	0.006	-	-
Fe^{3+}	0.588	0.613	0.648	0.666	0.749	0.641	0.721	0.753	0.963	1.959	1.982
Fe^{2+}	0.964	0.975	0.987	1.032	1.045	1.016	0.999	1.012	1.011	0.982	0.993
Mn	0.041	0.042	0.038	0.029	0.037	0.022	0.019	0.019	0.015	-	-
Ni	0.002	0.002	0.002	0.003	0.003	0.004	0.005	0.005	0.005	0.005	0.006
Zn	0.024	0.023	0.022	0.018	0.017	0.030	0.032	0.027	0.021	-	-
Mg	0.019	0.018	0.017	0.011	0.013	0.021	0.018	0.019	0.015	0.017	0.004
Σ cations	***3.000***	***3.000***	***3.000***	***3.000***	***3.000***	***3.000***	***3.000***	***3.000***	***3.000***	***3.000***	***3.000***
Σ O	***4.000***	***4.000***	***4.000***	***4.000***	***4.000***	***4.000***	***4.000***	***4.000***	***4.000***	***4.000***	***4.000***
C: Molecular-weight percent (end-member concentration in mol. %)											
$MgAl_2O_4$	1.30	1.20	1.15	0.85	0.65	0.80	0.70	0.80	0.60	-	-
$MgFe_2O_4$	0.60	0.60	0.55	0.25	0.65	1.30	1.10	1.10	0.90	1.70	0.40
$ZnFe_2O_4$	2.40	2.30	2.20	1.80	1.70	3.00	3.20	2.70	2.10	-	-
$MnFe_2O_4$	4.10	4.20	3.80	2.90	3.70	2.20	1.90	1.90	1.50	-	-
$NiFe_2O_4$	0.20	0.20	0.20	0.30	0.30	0.40	0.50	0.50	0.50	0.50	0.60
FeV_2O_4	0.35	0.40	0.40	0.50	0.55	0.35	0.35	0.35	0.30	-	-
Fe_2TiO_4	5.00	6.00	6.60	9.30	11.50	9.30	7.30	8.20	6.70	0.40	0.30
$FeCr_2O_4$	63.95	61.75	59.45	56.05	49.85	57.50	55.60	53.00	44.25	1.65	0.60
$FeFe_2O_4$	22.10	23.35	25.65	28.05	31.10	25.15	29.35	31.45	43.15	95.75	98.10
D: Calculated data											
Mg#	1.93	1.58	1.69	1.06	1.23	2.03	1.77	1.84	1.46	-	-
Cr#	98.01	98.09	98.10	98.51	98.71	98.63	98.76	98.51	98.66	-	-
Fe^{2+}/Fe^{3+}	1.64	1.59	1.52	1.55	1.40	1.59	1.39	1.34	1.05	0.50	0.50

Selected chromite analyses in talc schist (samples A 2 and TA 2) in wt. % (part A), apfu (part B) and in mol. % = end members concentration (part C). Ten analyses were carried out in the centre (columns IV and VIII XI) and two (columns VI and VII) in the higher reflecting rim of the crystals.

Table 2: Chemical composition of chromite in talc schist

	Talc-sample A 2							Talc-sample TA 2				
	I	**II**	**III**	**IV**	**V**	**VI_{rim}**	**VII_{rim}**	**VIII**	**IX**	**X**	**XI**	**XII**
A: Weight percent (wt. %)												
SiO_2	n.d.	0.14	n.d.	n.d.	n.d.	0.86	n.d.	0.24	n.d.	n.d.	n.d.	0.15
TiO_2	0.42	0.55	0.58	0.79	1.13	2.15	2.05	0.52	0.75	1.29	1.86	2.52
Al_2O_3	0.93	0.70	0.65	0.70	0.59	0.55	0.47	0.72	0.58	0.58	0.52	0.46
Cr_2O_3	56.76	54.37	53.86	50.50	46.96	41.73	40.94	57.35	53.47	51.30	46.46	43.00
V_2O_3	0.23	0.21	0.24	0.28	0.24	0.34	0.36	0.23	0.26	0.29	0.32	0.35
FeO_{anal}	37.65	39.26	40.75	43.33	45.97	51.00	51.95	36.87	40.85	42.62	46.38	49.30
MnO	0.61	0.69	0.69	0.71	0.77	0.53	0.50	0.57	0.63	0.66	0.69	0.52
NiO	n.d.	0.04	n.d.	0.06	0.05	0.13	0.13	0.04	n.d.	0.06	0.09	0.13
ZnO	1.22	1.25	1.19	1.14	1.17	0.96	0.82	1.43	1.49	1.35	1.26	1.04
MgO	0.75	0.64	0.66	0.61	0.40	0.47	0.33	0.43	0.35	0.30	0.33	0.22
FeO_{calc}	30.59	29.35	29.68	29.77	30.10	31.54	31.70	29.65	30.00	30.64	31.03	32.01
Fe_2O_{3calc}	7.85	11.01	12.30	15.07	18.74	21.63	22.50	8.03	12.06	13.32	17.06	19.99
Σ	***99.36***	***98.77***	***99.85***	***99.63***	***100.15***	***100.89***	***99.33***	***99.21***	***99.59***	***99.79***	***99.62***	***99.62***
B: Atoms per formula unit (apfu)												
Ti	0.012	0.016	0.016	0.022	0.032	0.061	0.058	0.015	0.021	0.036	0.053	0.071
Al	0.041	0.031	0.028	0.031	0.026	0.024	0.021	0.032	0.026	0.026	0.023	0.020
Cr	1.673	1.619	1.587	1.493	1.402	1.235	1.216	1.704	1.584	1.518	1.379	1.282
V	0.007	0.006	0.007	0.008	0.007	0.010	0.011	0.007	0.008	0.009	0.10	0.011
Fe^{3+}	0.255	0.312	0.345	0.424	0.501	0.609	0.636	0.227	0.340	0.375	0.482	0.545
Fe^{2+}	0.918	0.924	0.925	0.931	0.950	0.987	0.996	0.932	0.940	0.959	0.974	1.009
Mn	0.019	0.022	0.022	0.023	0.025	0.017	0.016	0.018	0.20	0.021	0.22	0.017
Ni	-	0.001	-	0.002	0.002	0.004	0.004	0.001	-	0.002	0.003	0.004
Zn	0.033	0.035	0.033	0.032	0.033	0.027	0.023	0.040	0.041	0.037	0.035	0.029
Mg	0.042	0.034	0.037	0.034	0.022	0.026	0.019	0.024	0.20	0.017	0.019	0.012
Σ cations	***3.000***	***3.000***	***3.000***	***3.000***	***3.000***	***3.000***	***3.000***	***3.000***	***3.000***	***3.000***	***3.000***	***3.000***
Σ O	***4.000***	***4.000***	***4.000***	***4.000***	***4.000***	***4.000***	***4.000***	***4.000***	***4.000***	***4.000***	***4.000***	***4.000***
C: Molecular-weight percent (end-member concentration in mol. %)												
$MgAl_2O_4$	2.05	1.55	1.40	1.55	1.30	1.20	1.05	1.60	1.30	1.30	1.15	1.00
$MgFe_2O_4$	2.15	1.85	2.30	1.85	0.90	1.40	0.85	0.80	0.70	0.40	0.75	0.20
$ZnFe_2O_4$	3.30	3.50	3.30	3.20	3.30	2.70	2.30	4.00	4.10	3.70	3.50	2.90
$MnFe_2O_4$	1.90	2.20	2.20	2.30	2.50	1.70	1.60	1.80	2.00	2.10	2.20	1.70
$NiFe_2O_4$	-	0.10	-	0.20	0.20	0.40	0.40	0.10	-	0.20	0.30	0.40
FeV_2O_4	0.35	0.30	0.35	0.40	0.35	0.50	0.55	0.35	0.40	0.45	0.50	0.55
Fe_2TiO_4	1.20	1.60	1.60	2.20	3.20	6.10	5.80	1.50	2.10	3.60	5.30	7.10
$FeCr_2O_4$	83.65	80.95	79.35	74.65	70.10	61.75	60.80	85.20	79.20	75.90	68.95	64.10
$FeFe_2O_4$	5.40	7.95	9.50	13.65	18.15	24.25	26.65	4.65	10.20	12.35	17.35	22.05
D: Calculated data												
Mg#	4.37	3.55	3.85	3.52	2.26	2.57	1.87	2.51	2.08	1.66	1.91	1.18
Cr#	97.61	98.12	98.27	97.97	98.18	98.09	98.30	98.16	98.39	98.32	98.36	98.46
Fe^{2+}/Fe^{3+}	3.60	2.97	2.68	2.20	1.90	1.62	1.57	4.11	2.77	2.56	2.02	1.85

Selected chromite (columns I to VIII) and magnetite (IX: chemically altered due to metamorphism And X and XI: newly-formed) analyses in serpentinite (samples SB 9 and NT 76) in wt. % (part A), apfu (part B) and in mol. % = end-member concentration (part C). The analyses were carried out in the centre of the crystals. End-members: spinel senso strict- $MgAl_2O_4$, magnesioferrite- $MgFe^{3+}{}_2O_4$, franklinite- $ZnFe^{3+}{}_2O_4$, ulvite- Fe_2TiO_4, jacobsite- $MnFe^{3+}{}_2O_4$ and trevorite- $NiFe^{3+}{}_2O$ chromite- $Fe^{2+}Cr_2O_4$, magnetite- $Fe^{2+}Fe^{3+}{}_2O_4$

Table 3: Chlorite in association with chromite in serpentine and talc schist

	Talc schist						Serpentinite			
	A 2			Ta 2			Sb 9		NT 76	
	I	II	III	IV	V	VI	VII	VIII	IX	X
A: Weight-percent (wt. %)										
SiO_2	32.06	32.74	33.40	32.11	32.15	32.88	30.69	31.08	33.40	33.94
TiO_2	0.07	-	-	-	-	-	-	-	-	-
Al_2O_3	13.53	12.83	12.65	13.43	13.31	12.84	15.62	15.63	12.35	11.25
Cr_2O_3	3.17	2.91	2.51	2.87	3.12	2.94	1.31	0.72	1.37	2.14
FeO_{anal}	6.56	6.29	6.56	6.81	6.51	6.72	8.45	8.04	6.18	6.25
MnO	-	0.05	-	-	-	-	-	-	-	-
NiO	0.18	0.29	0.22	0.23	0.14	0.25	0.16	0.13	0.22	0.20
MgO	32.20	31.66	32.19	32.00	32.05	31.81	30.81	30.57	32.54	32.36
CaO	-	0.06	-	-	-	-	-	-	-	0.07
Na_2O	-	-	-	-	-	-	-	0.04	-	-
K_2O	-	-	-	-	-	-	-	0.04	0.15	0.06
FeO_{calc}	5.69	6.29	6.56	5.99	5.97	6.72	6.31	6.75	5.93	6.25
Fe_2O_{3calc}	0.97	-	-	0.91	0.60	-	2.38	1.43	0.28	-
H_2O_{calc}	12.48	12.25	12.37	12.43	12.42	12.35	12.37	12.28	12.35	12.61
Σ	***100.35***	***99.08***	***99.90***	***99.97***	***99.76***	***99.79***	***99.65***	***98.57***	***98.59***	***98.88***
B: Atoms per formula unit (apfu)										
Si	3.077	3.178	3.213	3.095	3.102	3.175	2.972	3.033	3.241	3.306
A^{IV}	0.923	0.822	0.787	0.905	0.898	0.825	1.028	0.967	0.759	0.694
Σ	***4.000***	***4.000***	***4.000***	***4.000***	***4.000***	***4.000***	***4.000***	***4.000***	***4.000***	***4.000***
Al^{VI}	0.608	0.648	0.648	0.620	0.616	0.637	0.755	0.819	0.653	0.596
Ti	0.005	-	-	-	-	-	-	-	-	-
Cr	0.240	0.224	0.191	0.219	0.238	0.225	0.100	0.056	0.105	0.165
Fe^{3+}	0.070	-	-	0.066	0.044	-	0.173	0.105	0.020	-
Fe^{2+}	0.456	0.551	0.528	0.483	0.482	0.543	0.511	0.551	0.481	0.509
Mn	-	0.004	-	-	-	-	-	-	-	-
Ni	0.014	0.021	0.016	0.016	0.010	0.018	0.012	0.009	0.016	0.015
Mg	4.607	4.586	4.617	4.596	4.610	4.577	4.449	4.447	4.706	4.698
Ca		0.006	-	-	-	-	-	-	-	0.007
Na		-	-	-	-	-	-	0.008	-	-
K		-	-	-	-	-	-	0.005	0.019	0.008
Σ	***6.000***	***6.000***	***6.000***	***6.000***	***6.000***	***6.000***	***6.000***	***6.000***	***6.000***	***6.000***
Σ OH	8.000	7.950	7.948	8.000	8.000	7.963	8.000	8.000	8.000	7.939
Σ O	-	0.050	0.052	-	-	0.037	-	-	-	0.061
	8.000	***8.000***	***8.000***	***8.000***	***8.000***	***8.000***	***8.000***	***8.000***	***8.000***	***8.000***
C: Temperature calculation (Chathelineau I; Jowett II)										
I (°C)	235.3	202.7	191.5	229.5	227.2	203.7	269.1	249.4	182.5	161.5
II (°C)	228.3	228.9	196.4	222.7	220.5	197.6	262.5	243.0	176.1	155.5

Selected chlorite analyses in talc schist (samples A 2 and Ta 2) and serpentinite (samples Sb 9 and NT 76) in wt. % (part A) and apfu (part B) including the calculated temperature of chlorite formation after Chatelineau (1988) and Jowett (1991) (part C).

corresponding to 4 H_2O) and transformed into wt. % and added to the analytical sum (Table 3 under part A).

Petrography

Serpentinite

Serpentinite is typified by the samples NT 76 and SB 9. NT 76 is dark greenish in colour and contains chromite, magnetite, ilmenite, chalcopyrite, pyrrhotite and pentlandite. The minerals are fine grained and disseminated, and constitute more than 2 % of the rock volume. Chromite is the most abundant of the metallic minerals and has grain sizes of up to 200 x 60 ìm. The crystals are unzoned, irregularly developed and closely associated with chlorite that is concentrated along the rim often penetrating the chromite crystals (Fig. 3). Magnetite also occurs intergrown with chlorite, but shows slightly higher reflectivity than chromite. Ilmenite is rare and occurs as independent disseminations showing bireflection. Among the sulphides, chalcopyrite is the most abundant mineral. It is often intergrown with chromite (Fig. 4), but also with pyrrhotite that may contain exsolved pentlandite.

Serpentinite sample SB 9 is of light green colour. It contains small domains with rectangular to rounded outlines that contains abundant tiny and irregular shaped chromite crystals (distinctly smaller than 10 ìm in diameter). These crystals are always concentrated in small areas and are intergrown with, and embedded in a chlorite groundmass (Fig. 5). Rarely, chromite may also occur in the form of disseminated tiny crystals (5-10 ìm in diameter).

Fig. 3: Irregular shaped chromite crystal with corroded outlines is intergrown with chlorite (fine-grained needles, black). Chromite is embedded in chlorite which grades continuously into serpentinite (not visible under reflected light). Reflected light, oil immersion, length of the crystal 200 ìm. Serpentinite-sample NT 76.

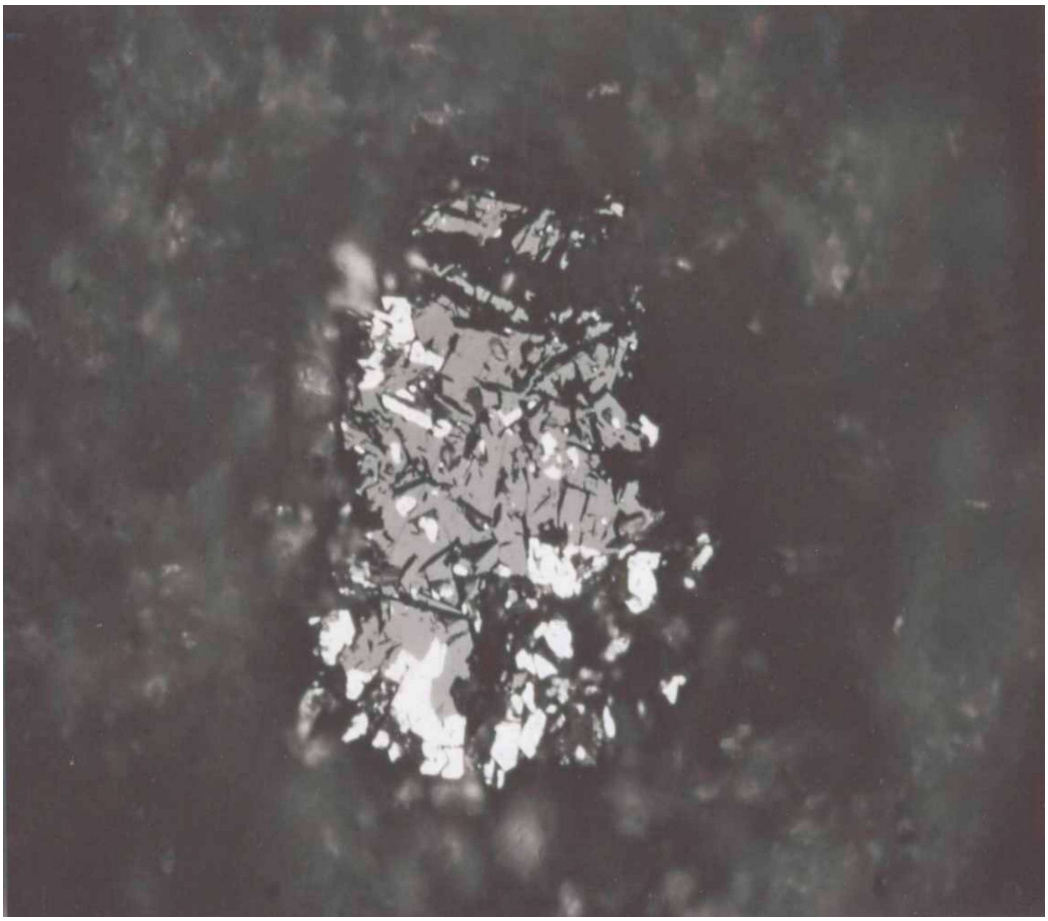

Fig. 4: Chromite (grey) intergrown with chalcopyrite (bright) and chlorite (needle-like and black) embedded in a small chlorite halo which grades continuously into a serpentine groundmass. Reflected light, oil immersion, diameter of the aggregate 150 ìm. Serpentinite-sample NT 76.

Talc schist

Talc schist, typified by samples A 2 and TA 2, is whitish to light grey in colour. It contains chromite as the only opaque mineral. This occurs in three varieties:

1. Similar to what obtains in serpentinite (sample SB 9), small chromite crystals may be concentrated in distinctly outlined areas (Fig. 6) that are recognisable in hand specimen by spots of dark colour impressions. The chromite crystals, especially those of bigger sizes (up to 80 ìm in diameter; Fig. 7), are zoned showing higher reflectivity along a very slim rim, as a sign of higher iron concentration relative to the core. Chromite is intimately intergrown with tiny and elongated chlorite crystals. The chromite rich areas are enveloped by a halo (in cm-dimension) that is dominated by chlorite which imparts a deeper greenish colour on such spots.
2. Chromite also occurs in the form of tiny crystals or aggregates that are regularly arranged to produce skeletal structures. One of such structures is akin to an ideally grown fir-tree with a strongly developed phylum in the centre and smaller obliquely arranged branches growing outward in both directions (= herringbone structure; Fig. 8).
3. Occassionally, chromite may also occur in the form of small (5 - 10 ìm in diameter) disseminated crystals.

Mineral chemistry

Chromite, magnetite and ilmenite

The analyses of chromite in serpentinite and talc schist are presented in the Tables 1 (columns I to VIII) and 2. These data are summarized in Figs. 9 and 10. Fig. 9 is the end-member diagram of chromite

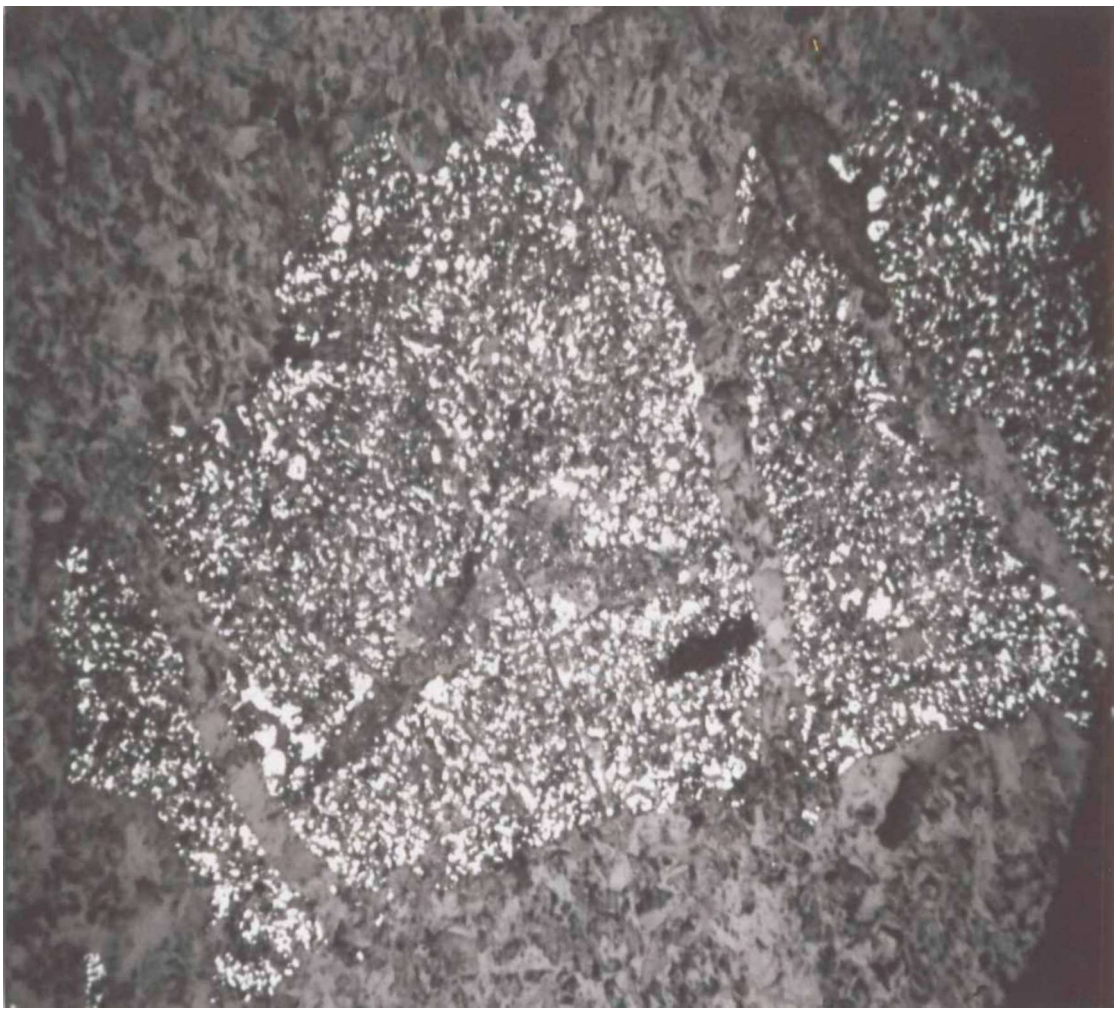

Fig. 5: Area occupied by a former compact chromite crystal in which tiny chromite crystals are now embedded in a groundmass of chlorite. Reflected light, diameter of the central aggregate 1.6 mm. Serpentinite-sample SB 9.

$Fe^{2+}Cr_2O_4$, magnetite $Fe^{2+}Fe^{3+}{}_2O_4$ and the sum of the other spinel end-members (spinel *senso stricto* $MgAl_2O_4$, magnesioferrite $MgFe^{3+}{}_2O_4$, franklinite $ZnFe^{3+}{}_2O_4$, ulvite Fe_2TiO_4, jacobsite $MnFe^{3+}{}_2O_4$ nalytical plots are arranged along a line ranging from high $Fe^{2+}Cr_2O_4$-concentrations to $Fe^{2+}Fe^{3+}{}_2O_4$-concentrations of about 50 mol.% which increase at the expense of $Fe^{2+}Cr_2O_4$. In one plot of sample NT 76 (arrowed in Fig. 9), the $Fe^{2+}Fe^{3+}{}_2O_4$-concentration is higher than that of $Fe^{2+}Cr_2O_4$ and is therefore, chromium rich magnetite (Table 1, part A, column IX). Fig. 9 also shows that the $Fe^{2+}Cr_2O_4$-concentration in the solid solutions are distinctly higher in the talc schist [represented with circle (= sample A 2) and square (= sample Ta 2)] than in serpentinite [represented with triangle (= sample NT 76) and star (= sample Sb 9)]. A compositional overlapping of the chromites from the two rocks however occurs. The plots of the two magnetite analyses from serpentinite (sample NT 76) are nearly pure $Fe^{2+}Fe^{3+}{}_2O_4$-solid solutions. As a sign of relatively high and nearly constant concentration of the other end-members in the chromite solid solutions (ranging between 12.6 and 19. 05 mol. % in serpentinite (Table 1, part D, column I IX) and 10.15 13.85 mol. % in talc schist (Table 2, part C), the plots deviate distinctly from the $Fe^{2+}Cr_2O_4$- $Fe^{2+}Fe^{3+}{}_2O_4$join, but are parallel to it.

Fig. 10 illustrates the compositional variations between franklinite $ZnFe^{3+}{}_2O_4$, ulvite Fe_2TiO_4 and the sum of the remaining end-members (spinel *senso stricto* $MgAl_2O_4$, magnesioferrite $MgFe^{3+}{}_2O_4$, jacobsite

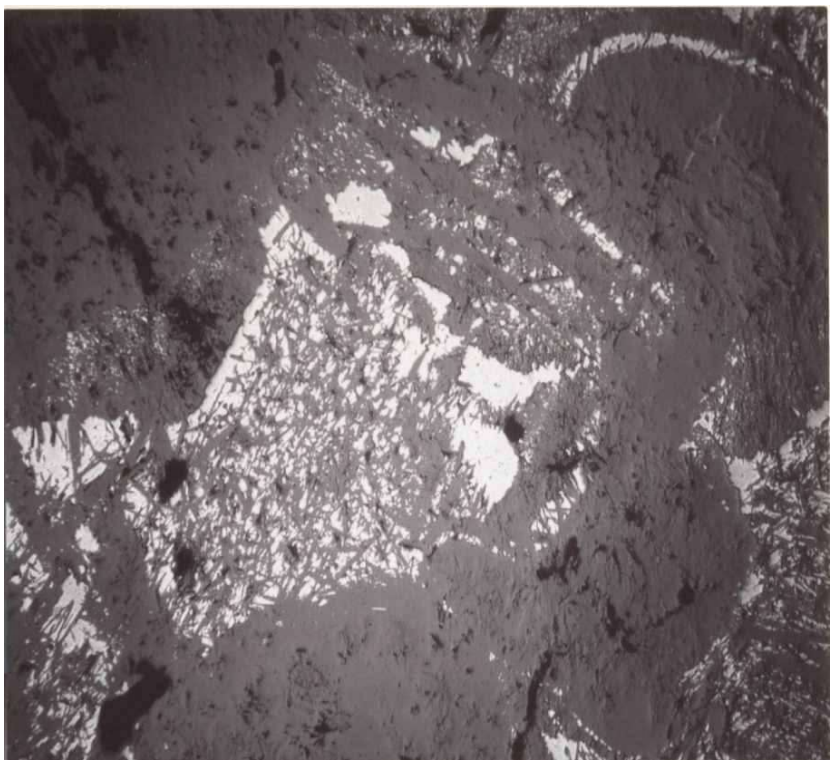

Fig. 6: Enrichment of tiny chromite crystal sometimes bigger along the rim within a rectangular outlined area of a former chromite crystal embedded in a chlorite groundmass. Reflected light, diameter of the chromite-bearing area 1 mm. Talc-sample A2.

Fig. 7: Enlarged position of Fig. 6 showing the bigger chromite crystals. These are zoned and intimately intergrown with needle-like chlorite crystals. Zonation is due to a small Fe-enrichment along the rim which shows slightly higher reflectivity than the Cr-richer core. The spots for analyses VI and VII of Table 2 are indicated with arrows. Reflected light, oil immersion, length of the two big crystals about 100 ìm. Talc-sample A

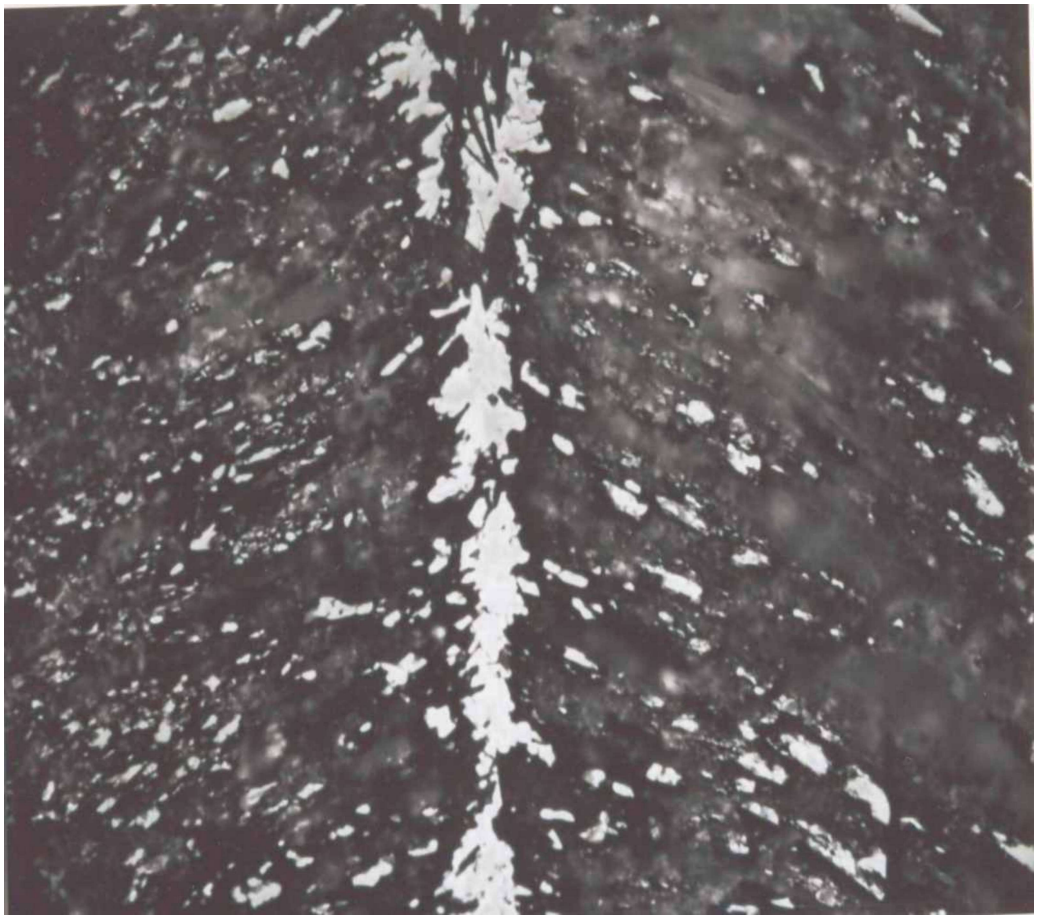

Fig. 8: Skeletal aggregates composed of bigger chromite crystals in the centre and tiny parallely arranged chromite crystals linked obliquely to the central 'phylum' (heringbone structure). The aggregate is embedded in chlorite intermixed with subordinate talc and anthophyllite. Reflected light, oil immersion, length of the central phylum 300 ìm. Talc-sample TA 2.

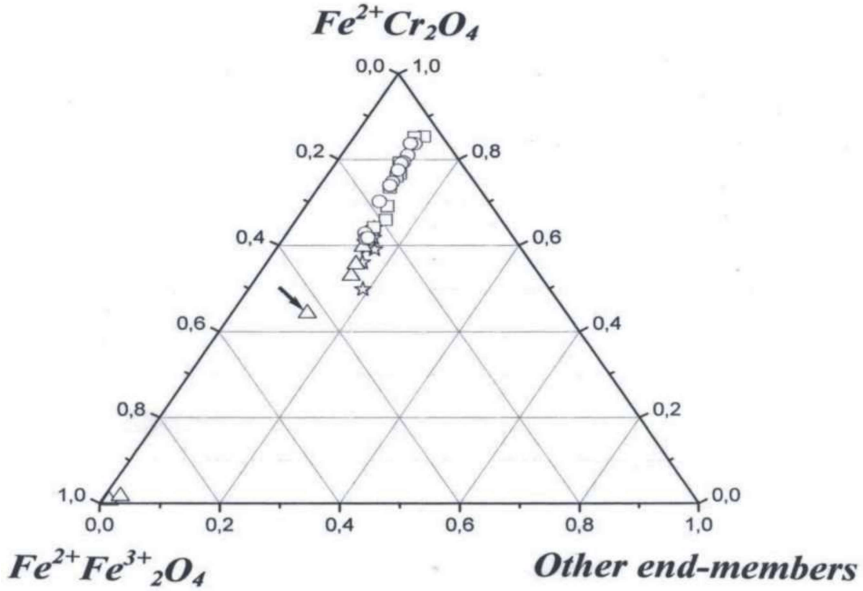

Fig. 9: Chromite ($Fe^{2+}Cr_2O_4$)-magnetite ($Fe^{2+}Fe^{3+}{}_2O_4$)-other end members - diagram containing the plots of chromite and magnetite solid solutions of serpentinite sample NT 76 (triangle) and Sb 9 (star) and of the talc schist samples A 2 (circle) and Ta 2 (quadrangle) . The diagram contains some plots, the analytical data of which are not published in the Tabs. 1 and 2.

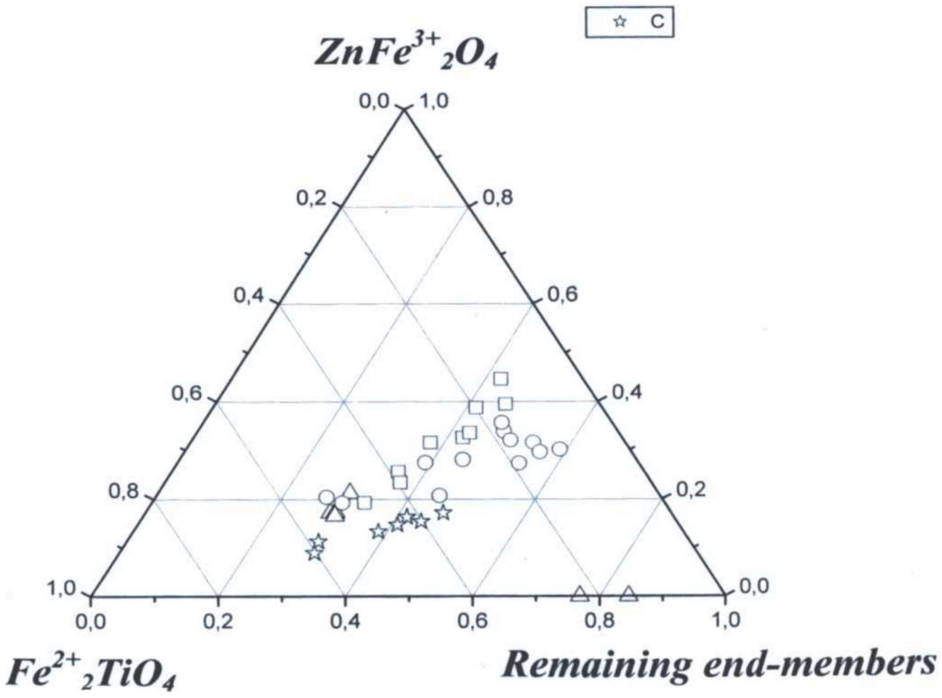

Fig. 10: Franklinite ($ZnFe^{3+}_2O_4$)-ulvite ($Fe^{2+}_2TiO_4$)-remaining end-members - diagram containing the plots of chromite and magnetite solid solutions of serpentinite sample NT 76 (triangle) and Sb 9 (star) and of the talc schist samples A 2 (circle) and Ta 2 (quadrangle). The diagram contains some plots the analytical data of which are not published in the Tabs. 1 and 2.

$MnFe^{3+}_2O_4$ and trevorite $NiFe^{3+}_2O_4$). The analytical plots from the different rock types plot separately, showing that the chromite solid solutions analysed in serpentinite [represented with triangle (= sample NT 76) and star (= sample Sb 9)] and talc schist [represented with circle (= sample A 2) and square (= sample Ta 2)] can easily be differentiated from one another: The analyses from serpentinite contain higher $ZnFe^{3+}_2O_4$ and remaining end-member concentrations than those from talc schist, which are partially slightly enriched in Fe_2TiO_4. The two magnetite plots from serpentinite-sample NT 76 lie on the Fe_2TiO_4 - remaining end-members join. A striking feature of all the chromite analyses is the low content of Al_2O_3 and MgO ranging from 0.26 to 0.93 wt. % in serpentinite (Tables 1, part A, columns I to VIII) and 0.19 to 0.75 wt. % in talc schist (Table 2, part A), respectively. Al_2O_3 and MgO are contained in the remaining end-members concentration and are calculated as $MgAl_2O_4$ and $MgFe^{3+}_2O_4$, the sum of which lies between 1.5 1.90 mol. % in serpentinite (Table 1, part D, column I VIII) and 1.2 4.2 mol. % in talc schist (Table 2, part D).

Ilmenite occurring in the same sample NT 76 has a solid solution composition consisting of the following end-members (in mol. %) : 92.2 to 92.4 ilmenite ($FeTiO_3$), 3.8 geikielite ($MgTiO_3$), 2.2 pyrophanite ($MnTiO_3$), 0.0 to 0.1 $NiTiO_3$, 1.25 to 1.7 Fe_2O_3 and 0.1 to 0.25 Cr_2O_3 (calculated from analyses not published).

Chlorite

The chlorite compositions of both serpentinite and talc schist are summarized in Table 3. Apart from serpentinite-sample Sb 9 (columns VII and VIII), the analytical data of the element oxides vary within a narrow range. These are in wt. % for SiO_2: 32.06 33.94, Al_2O_3: 11.25 13.53, FeO_{anal}: 6.18 6.81 and MgO: 31.66 32.54. In comparison with these data, the concentrations of Al_2O_3 and FeO are higher and those of MgO and SiO_2 are slightly lower in serpentinite-sample Sb 9 (Al_2O_3: 15.6, FeO: 8.04 and 8.45; MgO: 30.57 and 30.81 and SiO_2: 30.69 and 31.08; all data are in wt. %). Chlorite contains relatively high Cr_2O_3-concentrations in talc schist which range between 2.51 and 3.17 wt. %. They are lower in serpentinite varying from 0.72 2.14 wt. %. Although Ni is generally not a common constituent of chlorite, it is however enriched in all the analyzed chlorite crystals ranging between 0.13 and 0.29 wt. % (Table 3, part A).

Discussion

In the Isanlu area, the original chromite-bearing rocks and the original chromite composition are not preserved. However, chromite occurs in transformed ultramafic or mafic rocks that are either serpentinite or talc schist. The latter is far more abundant than the first. Remnants of primary silicate minerals and textures are also not preserved. It is well known, that under greenschist facies conditions of retrograde metamorphism, Mg-rich initial minerals (e. g. olivine and pyroxene) are often altered to Mg-rich hydrous silicates such as talc $Mg_3[(OH)_2/Si_4O_{10}]$ that may be associated with tremolite, chlorite and phlogopite (Wimmenauer, 1985). In SiO_2 undersaturated initial products, serpentinite is formed consisting predominantly of minerals of the serpentine-group $Mg_6[(OH)_8/Si_4O_{10}]$. Serpentinization is comparable with H_2O-metasomatism leading predominantly to the formation of water-rich minerals. A widespread phenomenon that is associated with both serpentinization and the formation of talc is CO_2-metasomatism that is documented by the occurrence of carbonates (calcite and magnesite) (Wimmenauer, 1985).

Concurrent with the transformation of silicates was the modification of the composition of pre-existing chromite . The analyzed chromite of this study occupy a narrow field (arrowed) on the Cr-number [=100Cr/(Cr + Al)] vs Mg-number [=100Mg/(Mg + Fe^{2+})] - diagram. This diagram also contains the compositional fields of chromite of stratiform (probable field of investigated chromite prior to its alteration) and podiform deposits after Steele *et al.,* (1977) (Fig. 11).

Previous studies in the Egbe-Isanlu schist belt of Olobaniyi (1997 and 2006) showed two distinct metamorphic imprints which he distinguished by means of structural and petrographic characteristics. The first was inferred to be related to the ca. 2000 Ma Eburnian event (Annor *et al.,* 1997 and Muecke, 2005) and the second is of Pan-African age been accompanied with the emplacement of the ca. 600 Ma granitoids (= Older Granite) of Nigeria. Olobaniyi (2006) discussed the metamorphic conditions of the two events leading to the mineral assemblages M_1 and M_2 resulting from pre-existing ultramafic rocks. M_1 was of mid-amphibolite facies under which high temperature sepentinization of the original ultramafic rocks occurred. This led apart from other minerals to

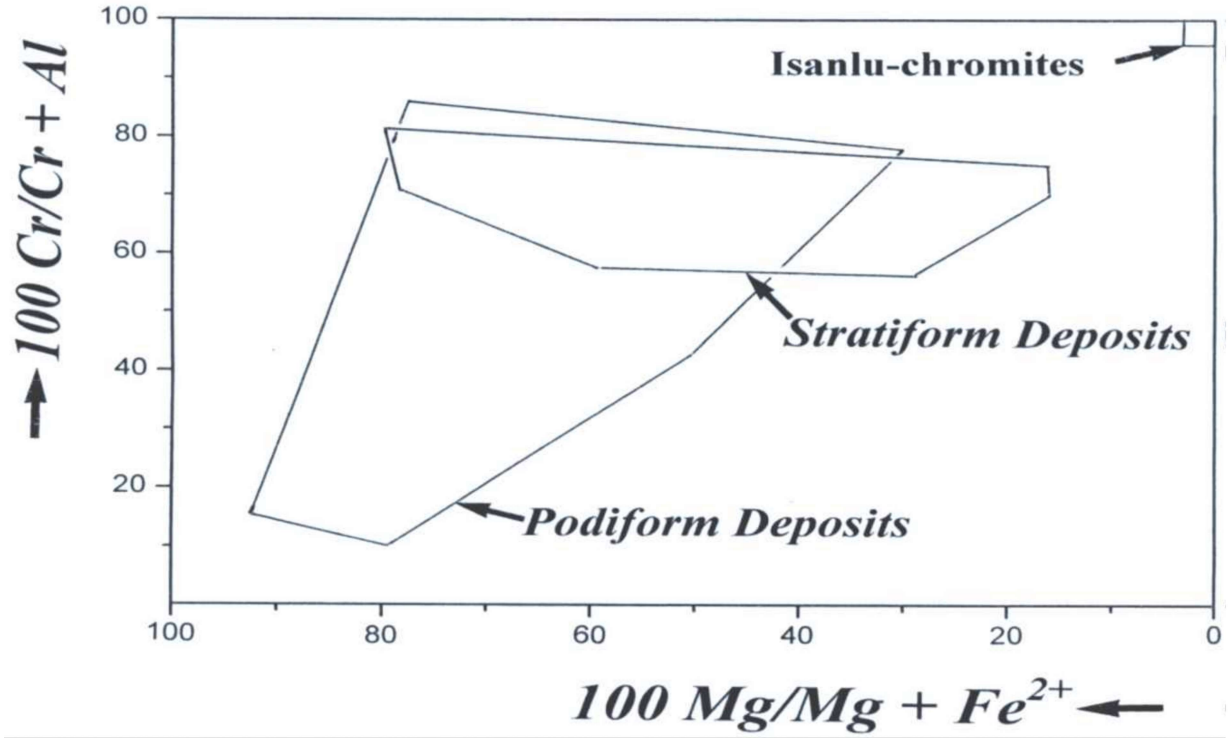

Fig. 11: Mg-number vs Cr-number - diagram including the compositional fields of stratiform and podiform chromite (after Steele et al., 1977) and the field of the investigated chromite solid solutions (arrowed).

the formation of antigorite. The M_2 was characterised by greenschist metamorphic conditions under which earlier assemblages probably suffered partial to total retrogression to produce talc rich assemblages. Other studies have also revealed that antigorite becomes unstable in favour of talc in the presence of silica- rich metamorphic-hydrothermal fluids (Hemley *et al.,* 1977), that accompanied the Pan-African event in the study area (Olobaniyi, 1997).

In mafic and ultramafic rocks, chromite undergoes chemical changes during metamorphism. These changes are presented in the Fe^{3+}-Cr-Al diagram of Evans and Frost (1975)(Fig. 12). This diagram considers the trivalent and therefore octahedral coordinated elements of the spinel structure only. Fig. 12 shows that low-grade metamorphosed spinel is enriched in Fe^{3+} and may occur as Cr-rich magnetite. With increasing grade of metamorphism, spinel becomes richer in chromium at the expense of Fe^{3+}, and finally, at high-grade metamorphism, both Cr and Al increase. Fig. 12 also contains the plots of the analyzed chromite crystals showing that they are Cr-rich especially those from talc schist. The plots are located exactly along the Fe^{3+} - Cr join, a deviation from the metamorphic path characterised by increasing Al_2O_3-concentations with increasing grade of metamorphism. The low Al_2O_3-concentation implies that the chemical composition of chromite apart from metamorphism was influenced by other conditions that occurred during serpentinization and talcitization. These conditions include the presence of H_2O-rich and CO_2-bearing fluids. These fluids are obviously responsible for the leaching not only of Al, but also of Mg from the original chromite crystals of all the investigated rock samples. As documented by many authors (e. g. Burkhard, 1993; Abzalov, 1998; Barnes, 2000; Wang et al., 2005; Proenza et al., 2008), leaching of Al and Mg is accompanied with an enrichment of iron in chromite in the form of Fe^{2+} instead of leached Mg and Fe^{3+} instead of leached Al. This accounts for the extremely high FeO_{calc}-concentrations ranging from 37.65 to 56.63 wt. % and low concentrations of Al_2O_3 (0.32 to 0.93 wt. %) and MgO (0.19 to 0.75 wt. %) in the investigated samples. The original chromite composition is unknown and therefore, the above mentioned elemental exchanges can only be inferred. Chromite from Maikwonaga (Anka schist belt) has FeO_{calc}-concentrations in the range between 23.71 and 25.20 wt. %. Those of MgO

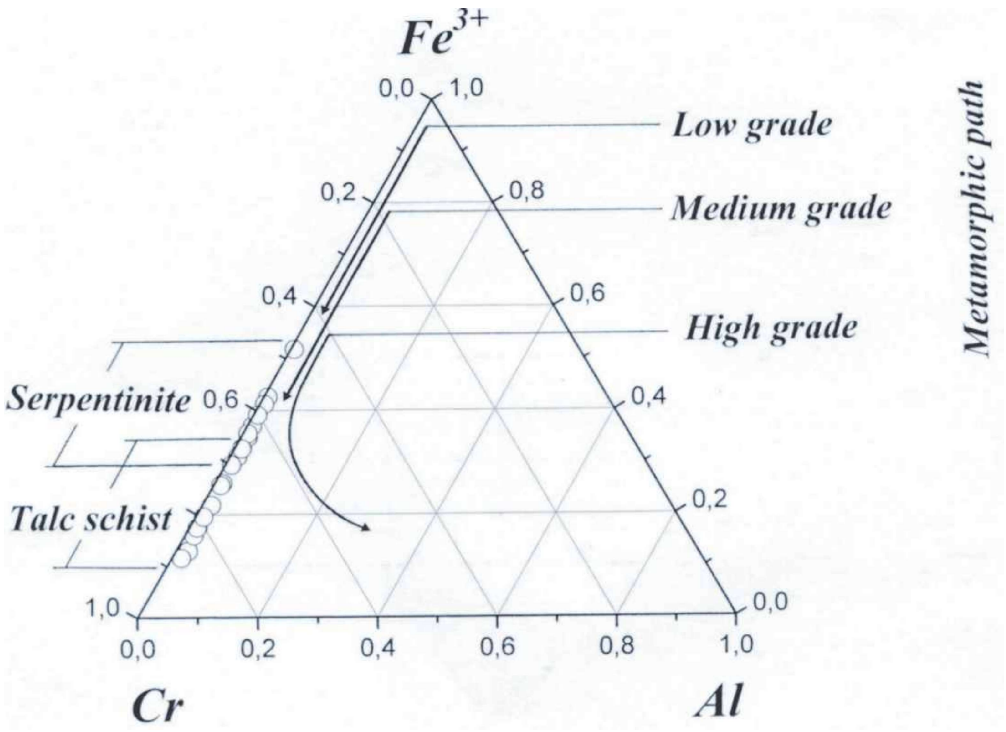

Fig. 12: Cr-Fe^{3+}-Al - diagram of chromite formed under various metamorphic conditions after Evans and Frost (1975) including the analytical plots of the investigated chromite crystals.

and Al_2O_3 vary from 6.20 to 7.33 wt. % and 10.5 to 14.5 wt. %, respectively (Mücke and Woakes, 1986). These values are similar to those of stratiform chromite of the Bushveld Igneous Complex (FeO_{calc}: 24.33 to 25.83 wt. %; MgO: 8.47 to 10.20 wt. %; and Al_2O_3: 14.49 16.67 wt. %)(Guilbert and Park, 1985). It is inferred that the original chromite composition of the investigated rocks was similar to chromite of the above mentioned deposits. This implies that iron concentration increased by more than 100 % and Mg and Al were nearly entirely leached during serpentinization and talcitization.

The concentration of TiO_2 in chromite varies within a wide range and has its highest value in serpentinite-sample SB 9 (4.03 wt. % TiO_2 or 11.50 mol. % $Fe^{2+}{}_2TiO_4$, Table 1, column V). The question of the origin of titanium, either contained in primary or enriched in secondary chromite cannot be simply answered. In Fig. 13 iron is presented in the form of magnetite ($Fe^{2+}Fe^{3+}{}_2O_4$) and titanium as ulvite ($Fe^{2+}{}_2TiO_4$) which are both contained in the investigated spinel-solid solution. The figure shows that the amount of ulvite increases which increasing magnetite concentration. This positive correlation is an indication that the Ti-content in chromite, at least partially is analogous to iron, also of secondary origin. It is also inferred that Ni was newly incorporated, originating probably from decomposing pentlandite $(Fe,Ni)_9S_8$. Zn which occurs in relatively high concentrations especially in chromite grains from talc schist has a highest value of 1.49 wt. % ZnO (Tab. 2, part A, column VIII) and may also be of secondary origin. This agrees with the work of Barnes (2000) who observed that elevated Zn-concentration in chromite is the result of Zn introduction during low temperature alteration with further concentration and homogenization during metamorphism.

In all samples, chromite is always intergrown with and/or embedded in chlorite (Figs. 3, 4 and 7). Chlorite is nearly constant in composition (Table 3) and identical with Mg-rich clinochlore (Fig. 14) which shows small variations in the Si-concentrations. Chlorite is enriched in Cr and Ni that are not characteristic constituents of chlorite. The content of Cr_2O_3 lies in the range between 2.51 and 3.17 wt. % in talc schist and between 0.72 and 2.14 wt. % in serpentinite (Table 3, columns I VI and columns VII X). The incorporation of these two elements in chlorite suggests that they were mobile in particularly in the talc schist during metasomatic alteration. The

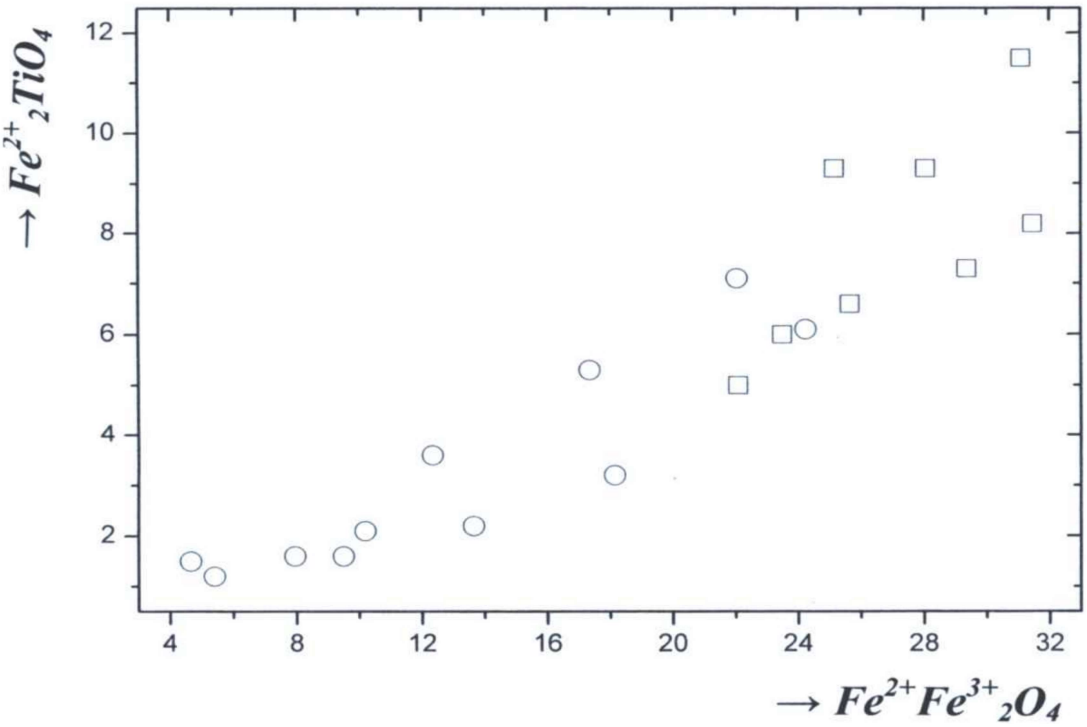

Fig. 13: Magnetite ($Fe^{2+}Fe^{3+}{}_2O_4$) vs ulvite ($Fe^{2+}{}_2TiO_4$) - diagram and the analytical plots of serpentinite (Quadrangle) and talc schist (circle).

temperature of formation of chlorite, which was calculated according to Chathelineau (1988) and Jowett (1991) are indicated under C of Table 3. These data show temperatures lying between 191.5 and 235.3 °C (Chathelineau) and 196.4 and 228.9 °C (Jowett) for chlorite contained in talc schist (columns I - VI), and between 249.4 and 269.1 °C (C) and 243 and 262.5 °C (J) for those of serpentinite-sample SB 9 (columns VII and VIII). The lowest temperatures were calculated for chlorite of serpentinite-sample NT 76 showing ranges from 161.5 to 182.5 °C (Chathelineau) and 155.5 to 176.1 °C (Jowett)(columns IX and X). All these low temperatures are indications, that chlorite was formed or re-equilibrated under retrograde conditions of the second metamorphic event. This low grade metamorphic event may also be responsible for further iron enrichment in chromite, caused by the continuation of Al and Mg leaching and accompanied with a decrease of the Cr_2O_3-concentration along a small and higher reflecting rim (Fig. 7; compare columns VI and VII with columns I to V of Table 2).

Conclusions

The parentage of the investigated chromite bearing serpentinite and talc schist is not unequivocally known because its primary silicate mineralogy is not preserved. However, the composition of chlorite is a useful indicator of the original environment (e. g. felsic, mafic and ultramafic) in which chlorite was formed. To characterize this environment, the diagram of Liard (1988) has been used (Fig. 15). The analytical plots of chlorite, having Mg-numbers which range between 0.893 and 0.910 and Al-numbers between 0.20 and 0.26, lie exactly in the ultramafic field. In agreement with other authors, it is concluded that the original rock was identical with the ultramafic rock type peridotite.

Further comparative studies within the Nigerian schist belts are necessary for comparison and should be carried out in the Anka schist belt where various chromite bearing rocks are exposed. These are the serpentinites of Mallam Tanko which are similar to those of the investigated rocks. The occurrences of Tugan Kudaku, Sado, Ribah and Maikwonaga (Wright and Ogezi, 1977, Muecke and Woakes, 1986 and Muecke, 2003) also contain chromite, but have distinctly higher ore mineral concentrations, bigger crystals and are less altered than the investigated rocks and those of Mallam Tanko. Analyses of ore minerals from Maikwonaga and Tugan Kudaku are mentioned

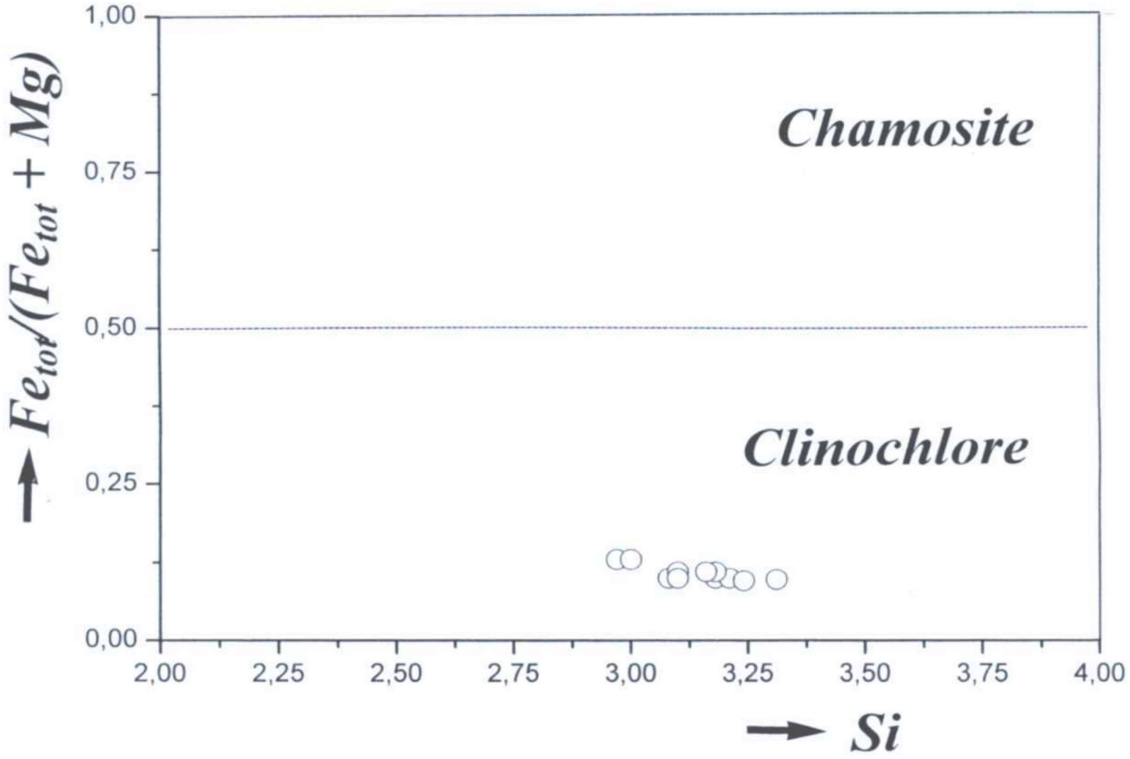

Fig. 14: Chlorite classification diagram [Cr vs $Fe_{tot}/(Fe_{tot} + Mg)$] modified after Melka (1965) showing the analytical plots of chlorite.

by Muecke and Woakes (1986) and Muecke (2003).

Acknowledgment

The electron- microprobe analyses were carried out in the Geochemical Institute, Centre of Geosciences, Georg-August-University of Göttingen, Germany by A. Kronz. We are very grateful to him. We are also grateful to the Editor-in-Chief Martin O. Eduvie and to two unknown reviewers for their comments and annotations.

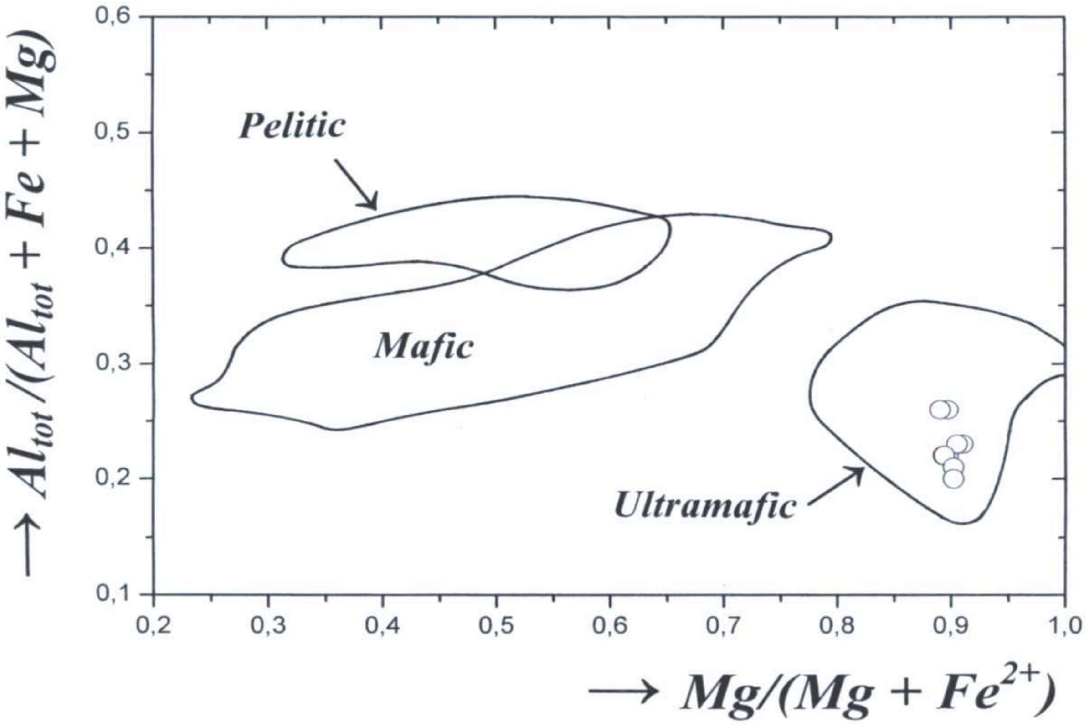

Fig. 15: Chlorite environmental classification diagram [Mg/(Mg + Fe) vs Al/(Al + Fe + Mg)] modified from Liard (1988) showing the analytical plots of chlorite

REFERENCES

ABZALOV, M. Z., 1998. Chrome-spinels in gabbro-wehrlite intrusions of the Pechenga area, Kola Peninsula, Russia: Emphasis on alteration features. Lithos 43, 109, 134.

ARIF, M and JAN, M.Q., 2006. Petrotectonic significance of the chemistry of chromite in the ultramafic complexes of Pakistan. Journal of Asian Earth Sciences, 27, pp. 628-646.

ANNOR, A. E., OLOBANIYI, S. B. and MÜCKE, A., 1997. Silicate facies iron-formation of the Egbe-Isanlu Palaeoproterozoic schist belt, southwest Nigeria. Journal African Earth Sciences 24, pp. 39-50.

AJIBADE, A. C., RAHAMAN, M. A. and WOAKES, M., 1987. Proterozioc crustal development in the Pan-African regime of Nigeria. In: Proterozoic lithospheric evolution (KRONER, A., ed.), American Geophysical Union 17, pp. 259-271.

BAER, H. P. and GLAESER, R., 1988. The Mallam Tanko serpentinites: Late-orogenic ultramafic intrusions in Pan-African Basement Complexes of NW-Nigeria. Precambrian Geology, Geological Survey of Nigeria, Kaduna: pp. 165-173.

BARNES, S., J., 2000. Chromite in komatiites, II. Modification during greenschist to mid-amphibolite facies metamorphism. Journal of Petrology 41, pp. 387- 409.

BARNES, S.J. and HILLS, R.E.T., 1995. Poikilitic chromite in komatiitic cumulates. Mineralogy and Petrology 54,pp. 85-92

BURKHARD, D., J., M., 1993. Accessory chromium spinels: Their coexistence and alteration in

serpentinites. Geochimica and Cosmochimica Acta 57, pp. 1297-1306.

CATHELINEAU, M., 1988. Cation site occupancy in chlorites and illites as a function of geothermometer. Clay Minerals 23, 471 485.

ELUEZE, A. A., 1981. Petrographic studies of metabasic rocks and meta-ultramafites in relation to mineralization in Nigerian schist belts. Journal of Mineralogy and Geology 19, pp. 21-29.

ELUEZE, A. A., 1982. Mineralogy and chemical nature of meta-ultramafites in Nigerian schist belts. Journal of Mineralogy and Geology 19, 21-29.

EVANS, B.W. and FROST, B.R., 1975. Chrom-spinel in progressive metamorphism: A preliminary analysis. Geochimimica and Cosmochimica Acta 39, pp. 959- 972.

GUILBERT, J. M., PARK Jr., C. F., 1985. The geology of ore deposits. W. H. Freeman and Company, New York, 377 pages.

HEMLEY, J.J., MONTOYA, J.W., SHAW, D.R. and LUCE, R.W., 1977. Mineral equilibria in the MgO-SiO_2-H_2O system: Talc-antigorite-forsterite-anthophyllite-enstatite stability relations and some geological implications in the systems. American Journal of Science 277, pp. 353-383

IGE, O. A. and ASUBIOJO, O. I., 1991. Trace element geochemistry and petrogenesis of some metaultramafites in Apomu of Ife-Ilesha areas of southwestern Nigeria. Chemical Geology 91, pp. 19-32.

JOWETT, E. C., 1991. Fitting iron and magnesium into the hydrothermal chlorite geothermometer. GAC/MAC/SEG Joint annual Meeting, Toronto 1991, Program with Abstracts, A62.

KAYODE, A. A., 1981. Komatiitic components in Ife-Ilesha amphibolite complex. 17th Ann. Conference of the Nigerian Mining and Geosciences Society, Calabar Abstract, pp. 37-38.

KLEMM, D. D., SCHNEIDER, W. and WAGNER, B., 1984. The Precambrian metavolcano-sedimentary sequence east of Ife and Ilesha southwest Nigeria: "A Nigerian greenstone belt ?". Journal of African Earth Sciences 2, pp. 161-176.

LIARD, J., 1988. Chlorites: metamorphic petrology. In BAILEY, S.W. (ed.): Hydrous phyllosilicates, Review in Mineralogy 19, pp. 405 447.

MELKA, K., 1965. Proposal of chlorite classification. Vest. Ústø. úst. geol. 40, pp. 23-29.

MUECKE, A., 2003. Magnetite, ilmenite and ulvite in rocks and ore deposits: petrography, microprobe analyses and genetic implications. Mineralogy and Petrology 77, pp. 215-234.

MUECKE, A., 2005. The Nigerian manganese-rich iron-formation and their host rocks from sedimentation to metamorphism. Journal of African Earth Sciences 41, pp. 407-436.

MUECKE, A. and WOAKES, M., 1986. Pyrophanite: a typical mineral in the Pan-African Province of Western and Central Nigeria. Journal of African Earth Sciences 5, pp. 675-689.

OGEZI, A. E. O., 1977. Geochemistry and geochronology of the basement rocks from the northwestern Nigeria. Ph. D. thesis, University of Leeds, 259 pages.

OGEZI, A. E. O., 1988. Geochemistry and origin of ensialic Alpine-type serpentinite associations from Mallam Tanko (Shemi) and Ribah (Wasagu), Northwestern Nigeria. Precambrian Geology, Geological Survey of Nigeria, Kaduna, pp. 257- 276.

OLOBANIYI, S.B., 1997. Geological and geochemical studies of the basement rocks and associated iron-formations of Isanlu area in the Egbe-Isanlu schist belt, Southwest Nigeria. Ph. D. thesis, University of Ilorin, Nigeria, 240 pages.

OLOBANIYI, S. B., 2006. Mineral chemistry and metamorphic conditions of Isanlu Amphibolites, southwest Nigeria. European Journal of Sciences and Research 13, pp. 119-131.

OLOBANIYI, S. B., 2008. Petrochemistry and tectonic setting of metabasic rocks of Isanlu, southwest Nigeria. Global Journal of Geological Sciences 6, pp. 113-122.

OLOBANIYI, S. B. and ANNOR, A. E., 2003. Petrology and age implication of ultramafic schist in the Isanlu area of the Egbe-Isanlu schist belt, southwestern Nigeria. Journal of Mining and Geology 39, pp. 1-9.

ONYEAGOCHA, A. C., 1979. The Mallam Tanko serpentinite: Petrology and economic implications. Journal of Mining and Geology

16 (1), pp. 37-40.

PROENZA, J. A., ZACCARINI, F., ESCOYOLA, M., CABANA, C., SCHALAMUK, A. and GARUTI, G., 2008. Composition and texture of chromite and platinum-group minerals in chromitites of the western ophiolitic belt from Pampean Ranges of Cordoba, Argentina. Ore Geology Reviews 33, pp. 32-48.

ROEDER, P.L., and CAMPBELL, I.H., 1985. The effect of post cumulus reactions on composition of chromite-spinel from the Jimberlain intrusion. Journal of Petrology 26, pp. 763-786.

STEELE, I. M., BISHOP, F. C., SMITH, J. V. and WINDLEY, B. F., 1977. The Fiskenaesset Complex, West Greenland, Part III. Grönlands geol. Unders. Bull. 124.

TRUSWELL, J. F. and COPE, R. N., 1963. The geology of parts of Niger and Zaria provinces, northern Nigeria. Bulletin of the Geological Survey, Nigeria, p.29.

WANG, C., Y., ZHOU, M-F. and ZHAO, D., 2005. Mineral chemistry of chromite from the Permian Jinboashan Pt-Pd-sulphide-bearing ultramafic intrusion in SW China with petrogenetic implications. Lithos 83, pp. 47 66.

WIMMENAUER, W. (1985): Petrographie der magmatischen und metamorphen Gesteine. Ferdinand Enke Verlag, Stuttgart, p. 156.

WRIGHT, J. B. and OGEZI, E. A. (1977): Serpentinite in the basement of northwestern Nigeria. Journal of Mining and Geology 14 (1), 34, 37.

Received 6th April, 2010, Revision accepted 7th June, 2011